The role of 18F-FDG PET/CT in predicting the pathological response to neoadjuvant PD-1 blockade in combination with chemotherapy for resectable esophageal squamous cell carcinoma

Xiaoyan Wang
  Sun Yat-sen University First Affiliated Hospital

Weixiong Yang
  Sun Yat-sen University First Affiliated Hospital

Qian Zhou
  Sun Yat-sen University First Affiliated Hospital

Hui Luo
  Sun Yat-sen University First Affiliated Hospital

Wenfang Chen
  Sun Yat-sen University First Affiliated Hospital

Sai-Ching Jim Yeung
  The University of Texas MD Anderson Cancer Center

Shuishen Zhang
  Sun Yat-sen University First Affiliated Hospital

Yi Gan
  Sun Yat-sen University First Affiliated Hospital

Bo Zeng
  Sun Yat-sen University First Affiliated Hospital

Zhenguo Liu
  Sun Yat-sen University First Affiliated Hospital

Shiting Feng
  Sun Yat-sen University First Affiliated Hospital

Xiangsong Zhang
  Sun Yat-sen University First Affiliated Hospital   https://orcid.org/0000-0003-3441-5194

Chao Cheng (✉ chengch3@mail.sysu.edu.cn)
  Sun Yat-sen University First Affiliated Hospital   https://orcid.org/0000-0003-3571-8154

Research Article

Posted Date: May 9th, 2022

Abstract

Purpose Accurate assessment of residual disease of tumor and lymph nodes after neoadjuvant immunochemotherapy is crucial in the active surveillance for patients with pathological complete response (pCR) and the optimal extent of lymphadenectomy for patients with non-pCR. This post-hoc analysis aimed to evaluate the performance of ^{18}F-FDG PET/CT to predict the pathological response to neoadjuvant immunochemotherapy for esophageal squamous cell carcinoma (ESCC).

Methods Fifty-eight resectable ESCC patients, received two cycles of camrelizumab in combination with chemotherapy were enrolled in the final analysis. The ^{18}F-FDG PET/CT scans were acquired at baseline (scan-1) and after immunochemotherapy but prior to surgery (scan-2). Maximum standardized uptake value (SUV_{max}), mean standardized uptake value (SUV_{mean}), tumor-to-blood pool SUV_{max} ratio (SUV_{TBR}), metabolic tumor volume (MTV) and total lesion glycolysis (TLG) were evaluated for their association with the pathological response to immunochemotherapy.

Results Nineteen patients (32.8%, 19/58) had pCR and thirty-nine patients (67.2%, 39/58) had non-pCR after two doses of camrelizumab and chemotherapy. At scan-2, the SUV_{max}, SUV_{mean}, SUV_{TBR}, TLG and MTV were significantly lower in pCR than that in non-pCR patients. Decrease in TLG and MTV between scan-2 and scan-1 of the same patient were significantly higher in the pCR than in the non-pCR group. In the receiver operating characteristic curve analysis, SUV_{max}, SUV_{mean}, SUV_{TBR}, TLG and MTV in scan-2 showed excellent predictive value for the pCR of primary tumors. Furthermore, SUV_{max} in scan-2 were higher in positive lymph nodes than that in negative ones, suggesting a high negative predictive ability (98.6%) with a cut-off value at 1.4.

Conclusion The parameters of ^{18}F-FDG PET/CT have the excellent performance for predicting pCR after the combined neoadjuvant immunochemotherapy in resectable ESCC.

Trial registration: ChiCTR ChiCTR2000028900. Registered 6 January 2020.

Introduction

Neoadjuvant chemoradiotherapy (nCRT) followed by surgery reportedly prolongs survival compared with surgery alone and has become the standard treatment for clinical stage II/III esophageal squamous cell carcinoma (ESCC) [1, 2]. Nonetheless, the clinical benefit of nCRT is still suboptimal and unsatisfactory due to the toxicity and increased risk of perioperative morbidity or mortality [3]. Emerging evidence showed the programmed cell death 1 (PD-1) blockade in combination with chemotherapy can induce optimal tumor regression and even bring a survival benefit to patients with advanced ESCC [4, 5]. Recently, we have conducted a clinical trial to examine the safety and feasibility of using the combination of neoadjuvant PD-1 blockade with chemotherapy in patients with ESCC, and found this regimen had good safety and favorable anti-tumor efficacy with a pathological complete response (pCR) of 25% [6]. Many studies have demonstrated that pCR is associated with a longer disease-free survival (DFS) and overall survival (OS) duration [7, 8]. In view of the substantial postoperative morbidity and the decrease of quality of life associated with esophagectomy, active surveillance approach could be implemented and improve outcomes in patients with pCR after neoadjuvant therapy [9]. Therefore, how to select patients achieving pCR after neoadjuvant immunochemotherapy is a

major unmet need in clinical practice. Moreover, classification of nodal metastases is also crucial for patients with non-pCR who need esophagectomy and lymphadenectomy. To clarify the positive and negative lymph nodes before surgery is helpful for the surgeon to perform limited lymph node dissection and decrease the postoperative complications associated with lymphadenectomy [10].

The conventional imaging modalities, such as computed tomography (CT), are only evaluated by using morphological imaging. It is difficult to distinguish viable tumors from necrotic or fibrotic tissue, resulting in the insufficient precision to reliably assess the response to neoadjuvant therapy in esophageal cancer (EC) [11]. Fluorine 18 (^{18}F)-fluorodeoxyglucose (FDG) positron emission tomography/computed tomography (PET/CT) can reflect the change in tumor metabolic activity and tumor viability independent of underlying structural changes by measuring the intensity of FDG uptake [12]. In EC, functional imaging using ^{18}F-FDG PET/CT can provide additional information of tumor metabolic that may eventually lead to therapeutic consequences [13]. Previous studies have found a direct association between maximum standardized uptake value (SUV_{max}) and pathological response to nCRT in patients with potentially resectable EC [14-16]. But the influence of immunotherapy on the intensity of FDG uptake in ^{18}F-FDG PET/CT remains unclear. The accuracy of response assessment in immunotherapy is radiologically challenging yet [17]. In recent studies, it was reported that ^{18}F-FDG PET/CT could predict pathological remission to the neoadjuvant immunotherapy in patients with resectable non-small cell lung cancer[18, 19]. To the best of our knowledge, there has been no evidence to support the effectiveness of ^{18}F-FDG PET/CT in evaluating the pathological response to the neoadjuvant immunochemotherapy for ESCC patients.

This study is based on an investigator-initiated, single-arm, prospective clinical trial of neoadjuvant PD-1 blockade in combination with nab-paclitaxel and carboplatin for resectable ESCC in our cancer center. This study was launched to address the knowledge gaps regarding on the relationship between tumor metabolic parameters of ^{18}F-FDG PET/CT and the pathological response to the neoadjuvant PD-1 blockade in combination with chemotherapy for resectable ESCC.

Materials And Methods

Study design and participants

A prospective, single-center, single-arm, investigator-initiated, clinical trial study, which was registered at http://www.chictr.org.cn/ (ChiCTR2000028900), was completed and reported (PMID: 35022193). The Ethics Committee of the First Affiliated Hospital of Sun Yat-sen University approved this prospective study and written informed consents were obtained from patients before PET/CT examinations. Eligible patients were 18-80 years old with pathologically or cytologically confirmed esophageal squamous cell carcinoma (stage II-IIIB, AJCC 8th edition) [20] that were surgically resectable. All patients had not received chemotherapy, radiotherapy or surgery related to esophageal cancer previously, with an Eastern Cooperative Oncology Group Performance Status of 0 or 1, and adequate organ function. Exclusion criteria were previous immunotherapy; known allergy to any monoclonal antibody or chemotherapy drug; active known autoimmune disease and symptomatic treatment of the disease or two years history before; known history of primary immunodeficiency; known active tuberculosis; severe and uncontrolled infections; congestive heart failure with grade III-IV; history of interstitial lung disease; uncontrolled hypertension; any arterial thromboembolic events occurred six months prior to

inclusion; significant malnutrition; or other primary malignant tumors. Patients had PET/CT examinations at various time points in the course of clinical care at the discretion of the primary oncology team and were not mandated by the clinical trial protocol. Patients who did not have PET/CT scans within one week prior to surgery (scan-2) were not included for further analysis.

Neoadjuvant Immunochemotherapy

The patients who were eligible to participate this clinical trial received two cycles of neoadjuvant PD-1 immunotherapy and chemotherapy before surgery: camrelizumab 200 mg, carboplatin (area under the curve [AUC]=5 mg/mL/min) and nab-paclitaxel (260 mg/m^2), that were administered intravenously on day 1 and day 22. Complete tumor resection was scheduled approximately 3-6 weeks after the first day of the second treatment cycle.

^{18}F-FDG PET/CT imaging

PET/CT examinations were performed from calvarium and mid-femur using an integrated PET/CT (Discovery MI, GE Healthcare). Patients were instructed to fast for at least 6 hours prior to their PET/CT scans, ensuring a normal blood glucose level in the range of 2.9-6.0 mmol/L. All patients rested for at least one hour after the intravenous injection of ^{18}F-FDG with a dose from 5.55 MBq/kg. The same scanning range CT (120 kV, 120-180 mA, slice thickness 1.25 mm) was acquired for anatomical localization and attenuation correction. PET imaging was performed from the acquisition in a three-dimensional mode with one minute per bed position. The scanning range was covered with six- to seven-bed positions. Then, the scan results were reconstructed using the super iterative algorithm.

Measurements of PET parameters

All images were observed and analyzed using PET volume computed assisted reading (PETVCAR) system, which is an automated segmentation software system with an Advantage Workstation (version 4.7; GE Healthcare). A volume-of-interest (VOI) around the whole tumor was auto-contoured and segmented using a boundary box. Two experienced nuclear medicine physicians would modify the VOI to ensure this 3-dimensional cube contained all the FDG-PET positive area and excluded the negative normal tissue in either of the axial, sagittal, and coronal planes. The following metabolic parameters of primary tumor were calculated by PETVCAR: maximum standardized uptake value (SUV$_{max}$), mean standardized uptake value (SUV$_{mean}$), metabolic tumor volume (MTV) and total lesion glycolysis (TLG). The SUV$_{max}$ of the blood pool was calculated using a round-shaped 10-mm in the aortic arch (without involving the vessel wall). Then the ratio of SUV$_{max}$ of primary tumor to SUV$_{max}$ of blood pool (SUV$_{TBR}$) were calculated. The post-treatment percentage changes of metabolic parameters were calculated as following (take ΔSUV$_{max}$% for example): ΔSUV$_{max}$% = (SUV$_{max}$ of scan-2 − SUV$_{max}$ of scan-1)/SUV$_{max}$ of scan-1 × 100%. Furthermore, SUVmax and short axis diameter (SAD) of the regional lymph node were recorded.

Pathological assessments

Pathological response was assessed by pathologists through measurement of the percentage of residual viable tumor after primary tumor resection, which was identified by routine hematoxylin and eosin staining.

Tumors without viable tumor cells were considered pathological complete response (pCR) [21]. The status of lymph node metastases was recorded.

Statistical analysis

Categorical variables were summarized with frequency and proportion. All data were verified for normal distribution with Shapiro-Wilk test and for homogeneity of variance with Levene's test. Normally distributed data were summarized as mean ± standard deviation (SD), median and range. The independent sample t test was used to compare them between two groups. Non-normally distributed data were summarized as the median and interquartile range (IQR). Mann-Whitney U tests were used to compare the metabolic parameters between two groups. The categorical variables were analyzed by chi-square or Fisher's exact test.

Tumor patients were categorized into the pCR and non-pCR groups according to their pathological outcomes. Receiver operating characteristic (ROC) curve analysis was used to evaluate the diagnostic performance and to determine the optimal cut-off value of each metabolic parameter to identify pCR patients. We also examined the performance of two PET/CT scans to identify positive lymph nodes in the lymph-node level using ROC analysis. Statistically significant factors in the univariate analysis were checked for collinearity using Spearman's rank correlation and variables that showed no collinearity with others (correlation coefficient less than 0.7) were fed into a multivariate binary logistic regression analysis [22]. The cut-off values for the ROC curve analysis were determined by the Youden index. Area under the ROC curve (AUC), sensitivity, specificity, positive predictive value (PPV), negative predictive value (NPV) and accuracy and their 95% confidence intervals (95% CIs) were estimated. Delong's test was used to compare two ROC curves. All data analyzes were performed using IBM SPSS Statistics for Windows, version 25.0 (IBMCorp, Armonk, N.Y., USA) [IBM Corp. Released 2017. IBM SPSS Statistics for Windows, version 25.0. Armonk, NY: IBM Corp.] and MedCalc for Windows, version 20.022 (MedCalc Software, Mariakerke, Belgium). Spearman's correlation coefficient was implemented in PerformanceAnalytics package from R version 4.1.3 (https://www.R-project.org/). All tests were two-sided and the statistical significance was set at P<0.05.

Results

Patient characteristics

From January 2020 to November 2021, a total of 81 patients with ESCC were screened for eligibility. Eventually, 79 eligible patients were enrolled (Fig. 1). The 79 patients received two cycles of neoadjuvant camrelizumab and chemotherapy. Twenty-one patients were excluded because twenty patients did not have PET/CT scans before surgery and one patient refused surgery. Finally, 58 patients were included in this analysis. Among the 58 patients, 19 patients (19/58, 32.8%) had pathological complete response (pCR), while the other 39 patients (39/58, 67.2%) did not. The patients had a median age of 59 years old, and most patients (46/59, 79.3%) were male. There was no significant difference in baseline characteristics and between pCR and non-pCR patients in terms of age, gender, smoking history, drinking history, clinical tumor stage, clinical lymph node stage and clinical stage (Table 1). The location of tumors was different between the pCR and non-pCR group (P=0.006). Among the pCR patients, 6 patients (6/19, 31.6%) had the tumor in upper esophagus, 8 patients (8/19, 42.1%) had the tumor in middle esophagus and the other 5 patients (5/19, 26.3%) had the tumor in lower esophagus. As for the non-pCR patients, 1 patient (1/39, 2.6%) had the tumor in upper esophagus, 20 patients (20/39,

51.3%) had the tumor in middle esophagus and the other 18 patients (18/39, 46.2%) had the tumor in lower esophagus. Of the 58 patients, 42 patients took ^{18}F-FDG PET/CT examination both at baseline (scan-1) and before surgery (scan-2), while the other 16 patients underwent ^{18}F-FDG PET/CT examination only before surgery (scan-2).

Tumor metabolic parameters of ^{18}F-FDG PET/CT prove a significant difference between pCR and non-pCR groups

At scan-1, there was no significant difference after Bonferroni correction in SUV_{max}, SUV_{mean}, SUV_{TBR}, MTV and TLG between the pCR and non-pCR groups (Table 2). All metabolic parameters of scan-2 were significantly lower in patients with pCR than in those with non-pCR (P<0.001, P<0.001, P<0.001, P=0.001 and P<0.001 for SUV_{max}, SUV_{mean}, SUV_{TBR}, MTV and TLG, respectively).

Delta TLG% and MTV% were significantly lower in the pCR group than that in the non-pCR group after neoadjuvant immunochemotherapy (P=0.003 and P=0.002). Delta SUV_{max}%, SUV_{mean}%, and SUV_{TBR}% showed no significant differences between the two groups (Table 2).

Tumor metabolic parameters of ^{18}F-FDG PET/CT predicts the therapeutic response of pCR

At scan-1, TLG (AUC, 0.716) and MTV (AUC, 0.721) discriminated pCR from patients with non-pCR. The following parameters at scan-2 corelated with pathological assessment discriminated pCR: SUV_{max} (AUC, 0.848), SUV_{mean} (AUC, 0.853), TLG (AUC, 0.850), MTV (AUC,0.856), and above all SUV_{TBR} (AUC, 0.860 [95%CI: 0.760, 0.959]; cut-off value, 2.1) providing 69.6% (16/23) PPV and 91.4% (32/35) NPV (Table 3, Supplemental Fig. 1), but the pairwise comparison ROC curve analysis among them didn't show difference in Delong's test (Supplemental table 1). At the percentage changes of delta TLG% (AUC, 0.762) and delta MTV% (AUC, 0.772) between scan-1 and scan-2 discriminated pCR from non-pCR patients (Table 3). According to the univariate analyses and correlation tests (Supplemental Fig. 2), metabolic parameters of PET scans were selected for inclusion in logistic regression models. The MTV of scan-1, SUV_{max} of scan-2 and ΔMTV% were included in binary logistic regression analysis to predict pCR. Independent variables in the regression models didn't indicate significant collinearity (variance inflation factor <10 and tolerance >0.1) in collinearity diagnostic test (Supplemental table 2). The multivariate logistic regression achieves AUC of 0.888, which is significantly higher than MTV of scan-1 (P=0.034) but didn't show significant difference with SUV_{max} of scan-2 or ΔMTV% (Table 3, Supplemental table 3, Supplemental Fig. 3). Fig. 2 (**a-f**) showed two representative cases patient with pCR and non-pCR.

PET/CT identified lymph node (LN) involvement

A total of 484 nodal stations from 58 participants were evaluated in our study (mean number of nodal stations sampled per patient: 8.3). Of these lymph nodes, 21 lymph node stations (21/484, 4.3%) in 12 patients (12/59, 20.7%) proved positive after surgery. At scan-1, SUV_{max} and SAD were significantly higher after Bonferroni correction in LN involvement (+) group than LN involvement (-) group (P=0.002 and P<0.001). At scan-2, SUV_{max} of lymph node were higher in the LN involvement (+) group than in the LN involvement (-) group but didn't show statistical significance after Bonferroni correction (P=0.009), while there was no significant

difference in SAD between LN involvement (+) and LN involvement (-) group. Delta SUV_{max}% and SAD% between scan-1 and scan-2 showed no significant difference between the two groups (Table 4).

From ROC analysis of scan-1, the optimal cut-off value for SUV_{max} (AUC, 0.733) and SAD (AUC, 0.769) distinguishing metastatic lymph nodes from benign ones was 4.8 and 6.5mm, respectively. However, ROC curve combined SUV_{max} and SAD didn't show difference with univariate ROC curves (Table 5, Supplemental table 4, Supplemental Fig. 4).At scan-2, the diagnostic performance of SUV_{max} (AUC, 0.746; cut-off value 1.4) to distinguish metastatic from benign nodes was significantly better than of SAD (AUC, 0.605; cut-off value 9.5) in the Delong's test (*P*=0.014), but combined ROC curves of them (AUC, 0.737) didn't show better diagnostic performance than SUV_{max} (*P*=0.333) (Table 5, Supplemental table 5, Supplemental Fig. 4). Moreover, there was no significant differences between the combined ROC curves of scan-1 and scan-2 (*P*=0.918). By setting the cut-off value of SUV_{max} of scan-2 at 1.4, the sensitivity, specificity, accuracy, PPV and NPV was 81.0% (17/21), 61.1% (283/463), 62.0% (300/484), 8.6% (17/197) and 98.6% (283/287), respectively (Table 5). Fig. 2 (**g-i**) showed a representative false-positive lymph node in FDG PET/CT imaging.

Discussion

To the best of our knowledge, this is the first study to report the role of ^{18}F-FDG PET/CT in predicting the pathological response to the neoadjuvant PD-1 blockade in combination with chemotherapy for the treatment of resectable ESCC. The major strengths of our study are its prospective nature, the use of well-standardized imaging and therapy protocols, as well as the direct correlation between ^{18}F-FDG PET/CT results and histopathology of the removed primary tumors and LNs. We found that metabolic parameters in scan-2 after treatment initiation was significantly associated with therapeutic response after two cycles of neoadjuvant immunochemotherapy treatment. The metabolic parameters in scan-2 showed high predictive performance for the pCR of primary tumors. Moreover, the SUV_{max} of scan-2 before surgery had good predictive performance for negative LNs (AUC, 0.746) with a NPV of 98.6%.

In our study, SUV_{max} (AUC 0.848, cut-off value 2.6), SUV_{mean} (AUC, 0.853; cut-off value 1.8) would predict pCR after two cycles of neoadjuvant immunochemotherapy with sensitivity of 73.7% (14/19) and 78.9% (15/19), specificity of 87.2% (34/39) and 82.1% (32/39) and PPV of 73.7% (14/19) and 68.2% (15/22), respectively, suggesting that ^{18}F-FDG PET/CT is efficient for predicting the pathological response of primary tumors. Previous systematic review and meta-analysis concluded that the efficacy of SUV_{max} in detecting residual disease after nCRT or neoadjuvant chemotherapy for EC is insufficient because the sensitivity, specificity and PPV was only 62%, 73% and 41%, respectively [23, 24]. Additionally, the overall classification accuracy of SUV_{max} in detecting residual disease after neoadjuvant immunochemotherapy (AUC, 0.848) in our study is also better than that of SUV_{max} in detecting residual disease after nCRT (AUC, 0.64-0.71) as reported previously [25, 26]. The radiation-induced esophagitis after nCRT can increased ^{18}F-FDG uptake, resulted in the high frequency of false positivity and limited diagnostic performance for detecting locoregional disease [27]. Compared with simple SUV_{max} and SUV_{mean} based on a pixel, the volume-based parameters such as TLG and MTV may be more meaningful in locally advanced ESCC, because they can reflect the metabolism of the entire tumor [28]. In our study, volume-based parameters had similarly favorable diagnostic performance, especially TLG (AUC, 0.850) and MTV (AUC, 0.856) after neoadjuvant therapy. Hence, we considered that metabolic parameters of

preoperative PET/CT scan might be a robust measurement of tumor metabolism for assessing the therapeutic efficacy of neoadjuvant immunochemotherapy in ESCC. The present study is valuable for future study to establish appropriate cut-off value for response assessment as well as to confirm an accurate SUV threshold for volumetric analysis in the prediction of pathologic response to neoadjuvant immunochemotherapy using PET/CT. Further studies with larger samples are required to validate the efficacy of ^{18}F-FDG PET/CT in predicting pCR to neoadjuvant immunochemotherapy in patients with ESCC.

Restaging the N stage after neoadjuvant therapy is a major challenge because the radiological appearances of lymph nodes after treatment are difficult to interpret due to induced fibrosis and necrosis. We also assessed the performance of ^{18}F-FDG PET/CT in predicting residual LNs after neoadjuvant immunochemotherapy in ESCC patients. Under the best cut-off value (1.4), SUV_{max} was found with high sensitivity (81.0%, 17/21) and low specificity (61.1%, 283/463) before the surgery in our study. In a systematic review and meta-analysis evaluating diagnostic accuracy for detecting regional lymph node response after nCRT for EC, SUV_{max} (<2.5) of PET/CT had high sensitivity (89.0%) and low specificity (50.0%), which was consistent from our results [24]. In our study, the NPV was high before the surgery (98.6%, 283/287), suggesting that lower SUV_{max} (<1.4) can predict low risk of tumor metastasis in LNs. On the other hand, given the low PPV (8.6%, 17/197), high false positive rate (38.9%, 180/463) and false negative rate (19.0%, 4/21), the accuracy of the PET/CT in predicting residual LNs (+) is insufficient. The combination of SUV_{max} and SAD could not improve the diagnostic ability of predicting residual LNs any more, as detected in our study. Further investigation is required to establish more suitable and efficient means for diagnosing residual LNs (+) after neoadjuvant immunochemotherapy in ESCC patients using multiple modalities. Of note, ^{18}F-anti-PD-L1, ^{89}Zr-nivolumab and ^{89}Zr-atezolizumab as immune-PET molecular imaging agents have been reported to offer possibility for assess tumor response to immunotherapy [29, 30]. Further explorations are needed to identify the value of immune-PET in assessing the response after neoadjuvant immunochemotherapy in ESCC.

Implementing an active surveillance strategy for patients with a pCR requires accurate assessment of residual disease after neoadjuvant treatment. Our study has revealed the excellent performance of preoperative ^{18}F-FDG PET/CT for predicting pCR to the neoadjuvant immunochemotherapy in resectable ESCC, suggesting that preoperative ^{18}F-FDG PET/CT could be a useful tool to select patients who would achieve pCR after neoadjuvant immunochemotherapy in clinical practice. The present study is also valuable for future clinical trials to establish appropriate SUV threshold and cut-off value for pCR assessment in the response to neoadjuvant immunochemotherapy using ^{18}F-FDG PET/CT in ESCC. Additionally, in ESCC patients with negative LNs evaluated by ^{18}F-FDG PET/CT before surgery, lymphadenectomy could be avoided in those negative LNs stations. It would be a hint for the thoracic surgeon to select the optimal extent of lymphadenectomy and perform limited lymph node dissection to minimize operative and post-operative complications.

The present study has some limitations. First, it was a single center study and the number of enrolled patients was small. Further studies with more samples are required to verify the efficacy of ^{18}F-FDG PET/CT in predicting the pathological response to neoadjuvant immunotherapy in ESCC patients. Second, the follow-up time was short and the median survival was not reached. We believe that longer follow-up period is needed to

examine whether PET parameters on primary tumors and lymph nodes could predict survival outcomes in patients with ESCC treated with neoadjuvant PD-1 blockade combined with chemotherapy followed by surgery.

In summary, the results of this study suggest that ^{18}F-FDG PET/CT is a useful tool for predicting the pathological response of primary tumors and LNs to neoadjuvant PD-1 blockade in combination with chemotherapy for resectable ESCC. Further studies with larger sample size would be beneficial to validate this conclusion and to examine whether pre-operative ^{18}F-FDG PET/CT after neoadjuvant immunochemotherapy is feasible to optimize lymph node dissection in the surgical resection with curative intent.

Abbreviations

pCR	pathological complete response
ESCC	esophageal squamous cell carcinoma
SUV_{max}	maximum standardized uptake value
SUV_{mean}	mean standardized uptake value
SUV_{TBR}	tumor-to-blood pool SUV_{max} ratio
MTV	metabolic tumor volume
TLG	total lesion glycolysis
nCRT	neoadjuvant chemoradiotherapy
PD-1	programmed cell death 1
DFS	disease-free survival
OS	overall survival
EC	esophageal cancer
^{18}F-FDG	fluorine 18- fluorodeoxyglucose
SAD	short axis diameter
IQR	interquartile range
ROC	receiver operating characteristic
AUC	area under the ROC curve
PPV	positive predictive value
NPV	negative predictive value
CI	confidence intervals
LN	lymph node

Declarations

Acknowledgments

Compliance with ethical standards

Conflict of interest

The authors declare no conflict of interest relevant to this study. Outside the context of this study, Dr. Yeung had prior grant funding from Bristol-Myer Squibb, Assertio (previously DepoMed) and Bausch Health, and participated in an expert panel for Celgene, Inc.

Ethical approval

All procedures performed in studies involving human participants were in accordance with the ethical standards of the Ethics Committee of the First Affiliated Hospital of Sun Yat-sen University and with the principles of the 1964 Declaration of Helsinki and its later amendments or comparable ethical standards as previously reported (PMID: 35022193).

Informed consent Informed consent was obtained from all patients enrolled in the study.

References

1. Shapiro J, van Lanschot JJB, Hulshof M, van Hagen P, van Berge Henegouwen MI, Wijnhoven BPL, et al. Neoadjuvant chemoradiotherapy plus surgery versus surgery alone for oesophageal or junctional cancer (CROSS): long-term results of a randomised controlled trial. Lancet Oncol. 2015;16:1090–8. doi:10.1016/S1470-2045(15)00040-6.

2. Yang H, Liu H, Chen Y, Zhu C, Fang W, Yu Z, et al. Neoadjuvant Chemoradiotherapy Followed by Surgery Versus Surgery Alone for Locally Advanced Squamous Cell Carcinoma of the Esophagus (NEOCRTEC5010): A Phase III Multicenter, Randomized, Open-Label Clinical Trial. J Clin oncology: official J Am Soc Clin Oncol. 2018;36:2796–803. doi:10.1200/jco.2018.79.1483.

3. Wang H, Tang H, Fang Y, Tan L, Yin J, Shen Y, et al. Morbidity and Mortality of Patients Who Underwent Minimally Invasive Esophagectomy After Neoadjuvant Chemoradiotherapy vs Neoadjuvant Chemotherapy for Locally Advanced Esophageal Squamous Cell Carcinoma: A Randomized Clinical Trial. JAMA Surg. 2021;156:444–51. doi:10.1001/jamasurg.2021.0133.

4. Kojima T, Shah MIA, Muro K, Francois E, Adenis A, Hsu CH, et al. Randomized Phase III KEYNOTE-181 Study of Pembrolizumab Versus Chemotherapy in Advanced Esophageal Cancer. J Clin Oncol. 2020;38. doi:10.1200/jco.20.01888.

5. Sun JM, Shen L, Shah MA, Enzinger P, Adenis A, Doi T, et al. Pembrolizumab plus chemotherapy versus chemotherapy alone for first-line treatment of advanced oesophageal cancer (KEYNOTE-590): a randomised, placebo-controlled, phase 3 study. Lancet. 2021;398:759–71. doi:10.1016/s0140-6736(21)01234-4.

6. Yang W, Xing X, Yeung S, Wang S, Chen W, Bao Y, et al. Neoadjuvant programmed cell death 1 blockade combined with chemotherapy for resectable esophageal squamous cell carcinoma. J Immunother Cancer. 2022;10. doi:10.1136/jitc-2021-003497.

7. Blum Murphy M, Xiao L, Patel V, Maru D, Correa A, Amlashi G. F, et al. Pathological complete response in patients with esophageal cancer after the trimodality approach: The association with baseline variables and survival-The University of Texas MD Anderson Cancer Center experience. Cancer. 2017;123:4106–13. doi:10.1002/cncr.30953.

8. Donahue J, Nichols F, Li Z, Schomas D, Allen M, Cassivi S, et al. Complete pathologic response after neoadjuvant chemoradiotherapy for esophageal cancer is associated with enhanced survival. The Annals of thoracic surgery. 2009;87:392-8; discussion 8–9. doi:10.1016/j.athoracsur.2008.11.001.

9. van der Wilk BJ, Noordman BJ, Neijenhuis LKA, Nieboer D, Nieuwenhuijzen GAP, Sosef MN, et al. Active Surveillance Versus Immediate Surgery in Clinically Complete Responders After Neoadjuvant Chemoradiotherapy for Esophageal Cancer: A Multicenter Propensity Matched Study. Ann Surg. 2021;274:1009–16. doi:10.1097/SLA.0000000000003636.

10. Hiranyatheb P, Osugi H. Radical lymphadenectomy in esophageal cancer: from the past to the present. Dis Esophagus. 2015;28:68–77. doi:10.1111/dote.12091.

11. Westerterp M, van Westreenen H, Reitsma J, Hoekstra O, Stoker J, Fockens P, et al. Esophageal cancer: CT, endoscopic US, and FDG PET for assessment of response to neoadjuvant therapy–systematic review. Radiology. 2005;236:841–51. doi:10.1148/radiol.2363041042.

12. Makino T, Yamasaki M, Tanaka K, Tatsumi M, Takiguchi S, Hatazawa J, et al. Importance of positron emission tomography for assessing the response of primary and metastatic lesions to induction treatments in T4 esophageal cancer. Surgery. 2017;162:836–45. doi:10.1016/j.surg.2017.06.007.

13. Schmidt T, Lordick F, Herrmann K, Ott K. Value of functional imaging by PET in esophageal cancer. J Natl Compr Cancer Network: JNCCN. 2015;13:239–47. doi:10.6004/jnccn.2015.0030.

14. Sánchez-Izquierdo N, Perlaza P, Pagès M, Buxó E, Rios J, Rubello D, et al. Assessment of Response to Neoadjuvant Chemoradiotherapy by 18F-FDG PET/CT in Patients With Locally Advanced Esophagogastric Junction Adenocarcinoma. Clin Nucl Med. 2020;45:38–43. doi:10.1097/rlu.0000000000002840.

15. Kukar M, Alnaji R, Jabi F, Platz T, Attwood K, Nava H, et al. Role of Repeat 18F-Fluorodeoxyglucose Positron Emission Tomography Examination in Predicting Pathologic Response Following Neoadjuvant Chemoradiotherapy for Esophageal Adenocarcinoma. JAMA Surg. 2015;150:555–62. doi:10.1001/jamasurg.2014.3867.

16. Metser U, Rashidi F, Moshonov H, Wong R, Knox J, Guindi M, et al. (18)F-FDG-PET/CT in assessing response to neoadjuvant chemoradiotherapy for potentially resectable locally advanced esophageal cancer. Ann Nucl Med. 2014;28:295–303. doi:10.1007/s12149-014-0812-2.

17. Lheureux S, Denoyelle C, Ohashi PS, De Bono JS, Mottaghy FM. Molecularly targeted therapies in cancer: a guide for the nuclear medicine physician. Eur J Nucl Med Mol Imaging. 2017;44:41–54. doi:10.1007/s00259-017-3695-3.

18. Tao XL, Li N, Wu N, He J, Ying JM, Gao SG, et al. The efficiency of F-18-FDG PET-CT for predicting the major pathologic response to the neoadjuvant PD-1 blockade in resectable non-small cell lung cancer. Eur J Nucl Med Mol Imaging. 2020;47:1209–19. doi:10.1007/s00259-020-04711-3.

19. Gao SG, Li N, Gao SY, Xue Q, Ying JM, Wang SH, et al. Neoadjuvant PD-1 inhibitor (Sintilimab) in NSCLC. J Thorac Oncol. 2020;15:816–26. doi:10.1016/j.jtho.2020.01.017.

20. Rice TW, Ishwaran H, Ferguson MK, Blackstone EH, Goldstraw P. Cancer of the Esophagus and Esophagogastric Junction: An Eighth Edition Staging Primer. J Thorac Oncol. 2017;12:36–42. doi:10.1016/j.jtho.2016.10.016.

21. de Gouw DJJM, Klarenbeek BR, Driessen M, Bouwense SAW, van Workum F, Futterer JJ, et al. Detecting Pathological Complete Response in Esophageal Cancer after Neoadjuvant Therapy Based on Imaging Techniques: A Diagnostic Systematic Review and Meta-Analysis. J Thorac Oncol. 2019;14:1156–71. doi:10.1016/j.jtho.2019.04.004.

22. Dormann CF, Elith J, Bacher S, Buchmann C, Carl G, Carre G, et al. Collinearity: a review of methods to deal with it and a simulation study evaluating their performance. Ecography. 2013;36:27–46. doi:10.1111/j.1600-0587.2012.07348.x.

23. Eyck BM, Onstenk BD, Noordman BJ, Nieboer D, Spaander MCW, Valkema R, et al. Accuracy of Detecting Residual Disease After Neoadjuvant Chemoradiotherapy for Esophageal Cancer: A Systematic Review and Meta-analysis. Ann Surg. 2020;271:245–56. doi:10.1097/SLA.0000000000003397.

24. de Gouw D, Klarenbeek BR, Driessen M, Bouwense SAW, van Workum F, Futterer JJ, et al. Detecting Pathological Complete Response in Esophageal Cancer after Neoadjuvant Therapy Based on Imaging Techniques: A Diagnostic Systematic Review and Meta-Analysis. J Thorac Oncol. 2019;14:1156–71. doi:10.1016/j.jtho.2019.04.004.

25. Hamai Y, Hihara J, Emi M, Furukawa T, Yamakita I, Kurokawa T, et al. Ability of Fluorine-18 Fluorodeoxyglucose Positron Emission Tomography to Predict Outcomes of Neoadjuvant Chemoradiotherapy Followed by Surgical Treatment for Esophageal Squamous Cell Carcinoma. Ann Thorac Surg. 2016;102:1132–9. doi:10.1016/j.athoracsur.2016.04.011.

26. Dewan A, Sharma S, Dewan A, Khurana R, Gupta M, Pahuja A, et al. Impact on Radiological and Pathological Response with Neoadjuvant Chemoradiation and Its Effect on Survival in Squamous Cell Carcinoma of Thoracic Esophagus. J Gastrointest cancer. 2017;48:42–9. doi:10.1007/s12029-016-9870-0.

27. Noordman BJ, Spaander MCW, Valkema R, Wijnhoven BPL, van Berge Henegouwen MI, Shapiro J, et al. Detection of residual disease after neoadjuvant chemoradiotherapy for oesophageal cancer (preSANO): a prospective multicentre, diagnostic cohort study. Lancet Oncol. 2018;19:965–74. doi:10.1016/s1470-2045(18)30201-8.

28. Choi Y, Choi JY, Hong TH, Choi YL, Oh D, Woo SY, et al. Trimodality therapy for locally advanced esophageal squamous cell carcinoma: the role of volume-based PET/CT in patient management and prognostication. Eur J Nucl Med Mol Imaging. 2022;49:751–62. doi:10.1007/s00259-021-05487-w.

29. Bensch F, van der Veen EL, Lub-de Hooge MN, Jorritsma-Smit A, Boellaard R, Kok IC, et al. (89)Zr-atezolizumab imaging as a non-invasive approach to assess clinical response to PD-L1 blockade in cancer. Nat Med. 2018;24:1852–8. doi:10.1038/s41591-018-0255-8.

30. Niemeijer AN, Leung D, Huisman MC, Bahce I, Hoekstra OS, van Dongen G, et al. Whole body PD-1 and PD-L1 positron emission tomography in patients with non-small-cell lung cancer. Nat Commun. 2018;9:4664. doi:10.1038/s41467-018-07131-y.

Tables

Table 1 Characteristics of the patients according to tumor pathological complete response.

Characteristic	All patients (n=58)	Patients with pCR (n=19)	Patients without pCR (n=39)	P value
Age (year)				0.445
Median (range)	59 (43, 79)	63 (48, 77)	58 (43, 79)	
Sex, no. (%)				1.000
Male	46 (79.3)	15 (78.9)	31 (79.5)	
Female	12(20.7)	4 (21.1)	8 (20.5)	
Smoking status, no. (%)				0.224
Never	28 (48.3)	7 (36.8)	21 (53.8)	
Former or current	30 (51.7)	12 (63.2)	18 (46.2)	
Drinking status, no. (%)				0.944
Never	37 (63.8)	12 (63.2)	25 (64.1)	
Former or current	21 (36.2)	7 (36.8)	14 (35.9)	
Clinical tumor stage, no. (%)				0.673
2	7 (12.1)	3 (15.8)	4 (10.3)	
3	51 (87.9)	16 (84.2)	35 (89.7)	
Clinical lymph node stage, no. (%)				0.954
N0	25 (43.1)	8 (42.1)	17 (43.6)	
N1	25 (43.1)	8 (42.1)	17 (43.6)	
N2	8 (13.8)	3 (15.8)	5 (12.8)	
Clinical stage, no. (%)				0.915
II	25 (43.1)	8 (42.1)	17 (43.6)	
III	33 (56.9)	11 (57.9)	22 (56.4)	
Tumor location in the esophagus, no. (%)				**0.006**
Upper third	7 (12.1)	6 (31.6)	1 (2.6)	
Middle third	28 (48.3)	8 (42.1)	20 (51.3)	
Lower third	23 (39.7)	5 (26.3)	18 (46.2)	
pCR, pathological complete response.				

Table 2 Characteristics of metabolic parameters according to tumor pathological complete response

Metabolic parameters	pCR Median and IQR	non-pCR Median and IQR	z value	P value
Scan-1[a]				
SUV_{max}	14.7 (6.5, 21.6)	16.6 (11.6, 22.7)	-1.412	0.158
SUV_{mean}	9.6 (3.7, 14.3)	10.3 (7.4, 13.6)	-1.205	0.228
SUV_{TBR}	11.4 (5.3, 17.5)	11.2 (8.1, 19.4)	-1.088	0.277
TLG	44.4 (18.3, 104.8)	105.2 (50.4, 210.5)	-2.331	0.020
MTV	6.5 (2.7, 9.8)	11.5 (5.9, 21.5)	-2.383	0.017
Scan-2[b]				
SUV_{max}	2.0 (1.7, 2.9)	4.7 (2.8, 9.0)	-3.678	**<0.001**
SUV_{mean}	1.5 (1.2, 1.7)	2.9 (1.9, 5.2)	-3.512	**<0.001**
SUV_{TBR}	1.7 (1.4, 1.2)	4.4 (2.3, 6.0)	-4.144	**<0.001**
TLG	0.0 (0.0, 0.0)	3.8 (1.5, 19.0)	-3.364	**0.001**
MTV	0.0 (0.0, 0.0)	2.2 (0.8, 6.1)	-3.525	**<0.001**
The percentage changes (Δ%) between scan-1 and scan-2[a]				
$\Delta SUV_{max}\%$	-74.6 (-89.6, -64.9,)	-72.6 (-85.0, -53.2)	-1.476	0.140
$\Delta SUV_{mean}\%$	-73.1 (-89.5, -56.2)	-71.6 (-82.4, -56.0)	-1.269	0.204
$\Delta SUV_{TBR}\%$	-81.9 (-89.4, -46.1)	-60.2 (-79.0, -48.3)	-1.813	0.070
$\Delta TLG\%$	-100.0 (-100.0, -97.4)	-93.4 (-99.6, -84.7)	-2.921	**0.003**
$\Delta MTV\%$	-100.0 (-100.0, -93.6)	-81.3 (-96.5, -49.4)	-3.029	**0.002**

pCR, pathological complete response; IQR, interquartile range; SUV_{max}, maximum standardized uptake value; SUV_{mean}, mean standardized uptake value; SUV_{TBR}, the tumor-to-blood pool SUV_{max} ratio; MTV, metabolic tumor volume; TLG, total lesion glycolysis.

a n=42, including 16 patients with pCR and 26 patients with non-pCR; **b** n=58, including 19 patients with pCR and 39 patients with non-pCR.

Bold font indicates statistical significance after Bonferroni correction (i.e, $P<0.003$)

Table 3 Values of the metabolic parameters on predicting tumor pathological complete response.

	AUC, estimate (95%CI)	Cut-off value	Positive diagnostic test	Sensitivity %	Specificity %	Accuracy %	PPV %	NPV %
Scan-1								
SUV_{max}	0.631 (0.445, 0.817)	8.1	<	37.5	100.0	76.2	100.0	72.2
SUV_{mean}	0.612 (0.419, 0.805)	5.0	<	37.5	100.0	76.2	100.0	72.2
SUV_{TBR}	0.601 (0.413, 0.789)	7.0	<	37.5	96.2	73.8	85.7	71.4
TLG	0.716 (0.555, 0.877)	58.3	<	68.8	73.1	71.4	61.1	79.2
MTV	0.721 (0.565, 0.877)	13.5	<	93.8	46.2	64.3	51.7	92.3
Scan-2								
SUV_{max}	**0.848 (0.745, 0.951)**	2.6	<	73.7	87.2	82.8	73.7	87.2
SUV_{mean}	**0.853 (0.751, 0.955)**	1.8	<	78.9	82.1	81.0	68.2	88.9
SUV_{TBR}	**0.860 (0.760, 0.959)**	2.1	<	84.2	82.1	82.8	69.6	91.4
TLG	**0.850 (0.746, 0.953)**	1.2	<	84.2	82.1	82.8	69.6	91.4
MTV	**0.856 (0.752, 0.961)**	0.4	<	84.2	84.6	84.5	72.7	91.7
The percentage changes (Δ%) between scan-1 and scan-2								
$\Delta SUV_{max}\%$	0.637 (0.457, 0.817)	-88.3	<	37.5	96.2	73.8	85.7	71.4
$\Delta SUV_{mean}\%$	0.618 (0.430, 0.806)	-86.2	<	43.8	92.3	73.8	77.8	72.7
$\Delta SUV_{TBR}\%$	0.668 (0.485, 0.851)	-84.7	<	50.0	92.3	76.2	80.0	75.0

	AUC (95% CI)	Cut-off						
ΔTLG%	0.762 (0.601, 0.923)	-99.9	<	75.0	80.8	78.6	70.6	84.0
ΔMTV%	0.772 (0.615, 0.928)	-99.3	<	75.0	80.8	78.6	70.6	84.0
Multivariable*	0.888 (0.789, 0.987)	0.462[#]	>	87.5	80.8	83.3	73.7	91.3

AUC, area under the ROC curve; PPV, positive predictive value; NPV, negative predictive value; SUV_{max}, maximum standardized uptake value; SUV_{mean}, mean standardized uptake value; SUV_{TBR}, the tumor-to-blood pool SUV_{max} ratio; TLG, total lesion glycolysis; MTV, metabolic tumor volume.

*Multivariable: including MTV of scan-1, SUV_{max} of scan-2 and ΔMTV%.

[#]The cut-off value determined by Youden index in multivariable binary logistic regression analysis.

Table 4 Characteristics of lymph node (LN) stations (n=484) from 58 patients according pathological involvement.

	LN involvement (+) Median and IQR	LN involvement (-) Median and IQR	z value	P value
Scan-1[a]				
SUV_{max}	3.6 (1.4, 8.0)	1.4 (1.0, 2.0)	-3.162	**0.002**
SAD (mm)	8.0 (6.3, 10.0)	5.0 (4.0, 6.0)	-3.694	**<0.001**
Scan-2[b]				
SUV_{max}	1.7 (1.4, 3.4)	1.2 (0.8, 1.6)	-3.824	0.009
SAD (mm)	5.0 (4.0, 9.0)	5.0 (4.0, 6.0)	-1.663	0.096
The percentage changes (Δ%) between scan-1 and scan-2[a]				
ΔSUV_{max}%	2.8 (-61.5, 34.8)	-17.9 (-45.9, 14.6)	-0.488	0.625
ΔSAD%	-14.3 (-48.6, 8.3)	0.0 (-16.7, 0.0)	-1.653	0.098

IQR, interquartile range; SUV_{max}, maximum standardized uptake value; SAD, short axis diameter.

[a] n=374, including 16 lymph node stations involvement and 358 lymph node stations without involvement from 31 patients; [b] n=484, including 21 lymph node stations involvement and 463 lymph node stations without involvement from 38 patients.

Bold font indicates statistical significance after Bonferroni correction (i.e, $P<0.008$)

Table 5 Values of the metabolic parameters on predicting lymph node involvement.

	AUC, estimate (95%CI)	Cut-off value	Positive diagnostic test	Sensitivity %	Specificity %	Accuracy %	PPV %	NPV %
Scan-1								
SUV_{max}	0.733 (0.586, 0.880)	4.8	>	50.0	95.5	93.6	33.3	97.7
SAD	0.769 (0.633, 0.905)	6.5	>	75.0	76.0	75.9	12.2	98.6
SUV_{max}+SAD	0.770 (0.631, 0.908)	0.036*	>	75.0	72.9	73.0	11.0	98.5
Scan-2								
SUV_{max}	0.746 (0.644, 0.849)	1.4	**>**	81.0	61.1	62.0	8.6	98.6
SAD	0.605 (0.467, 0.743)	9.5	>	23.8	97.4	94.2	29.4	96.6
SUV_{max}+SAD	0.737 (0.629, 0.845)	0.462*	>	76.2	61.1	61.8	8.2	98.3
The percentage changes (Δ%) between scan-1 and scan-2								
ΔSUV_{max}%	0.536 (0.358, 0.714)	21.4	>	43.8	77.4	75.9	8.0	96.9
ΔSAD%	0.618 (0.442, 0.794)	-43.7	<	31.3	97.2	94.4	33.3	96.9

AUC, area under the ROC curve; PPV, positive predictive value; NPV, negative predictive value; SUV_{max}, maximum standardized uptake value; SAD, short axis diameter.

*The cut-off value determined by Youden index in binary logistic regression analysis
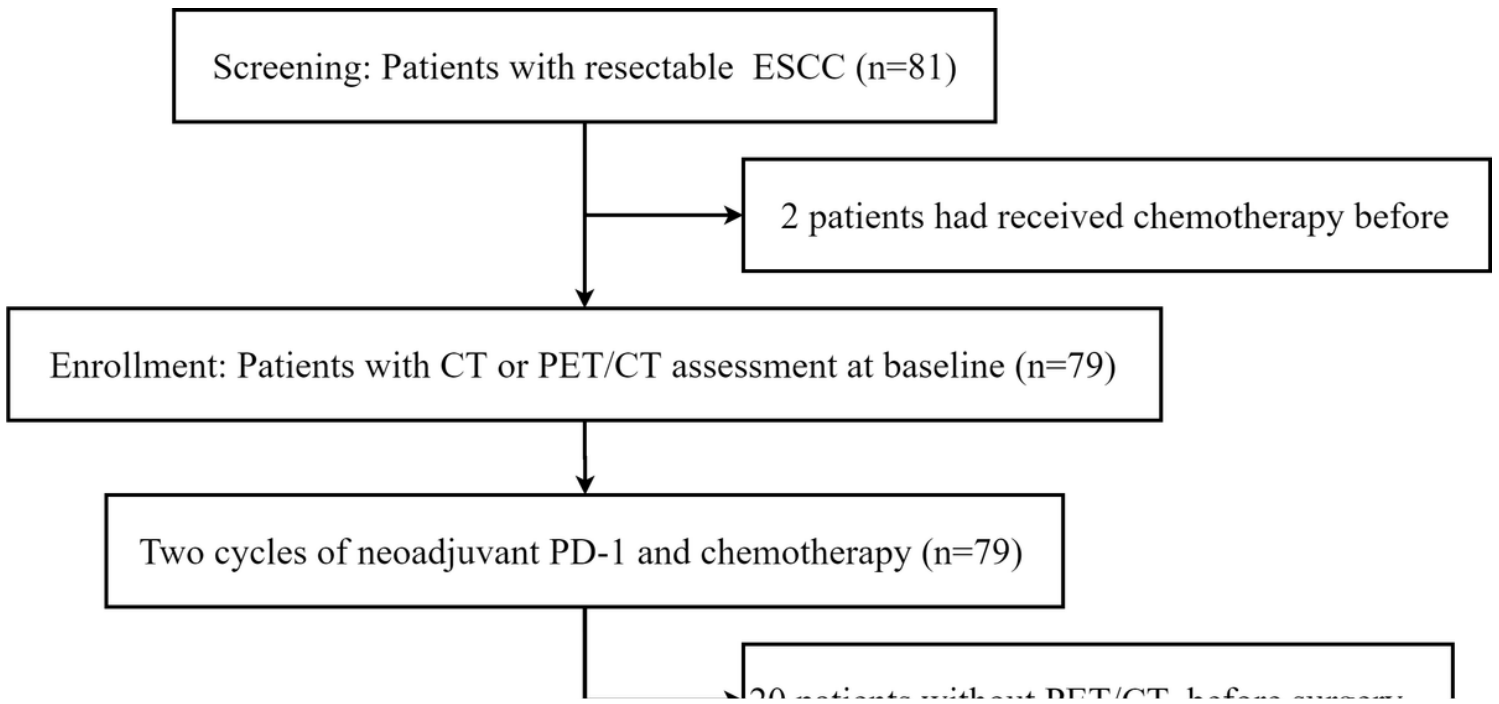
Figures

Figure 1

Flowchart of the study. pCR, pathologic complete response; CT, computed tomography; PET/CT, positron emission tomography/computed tomography.
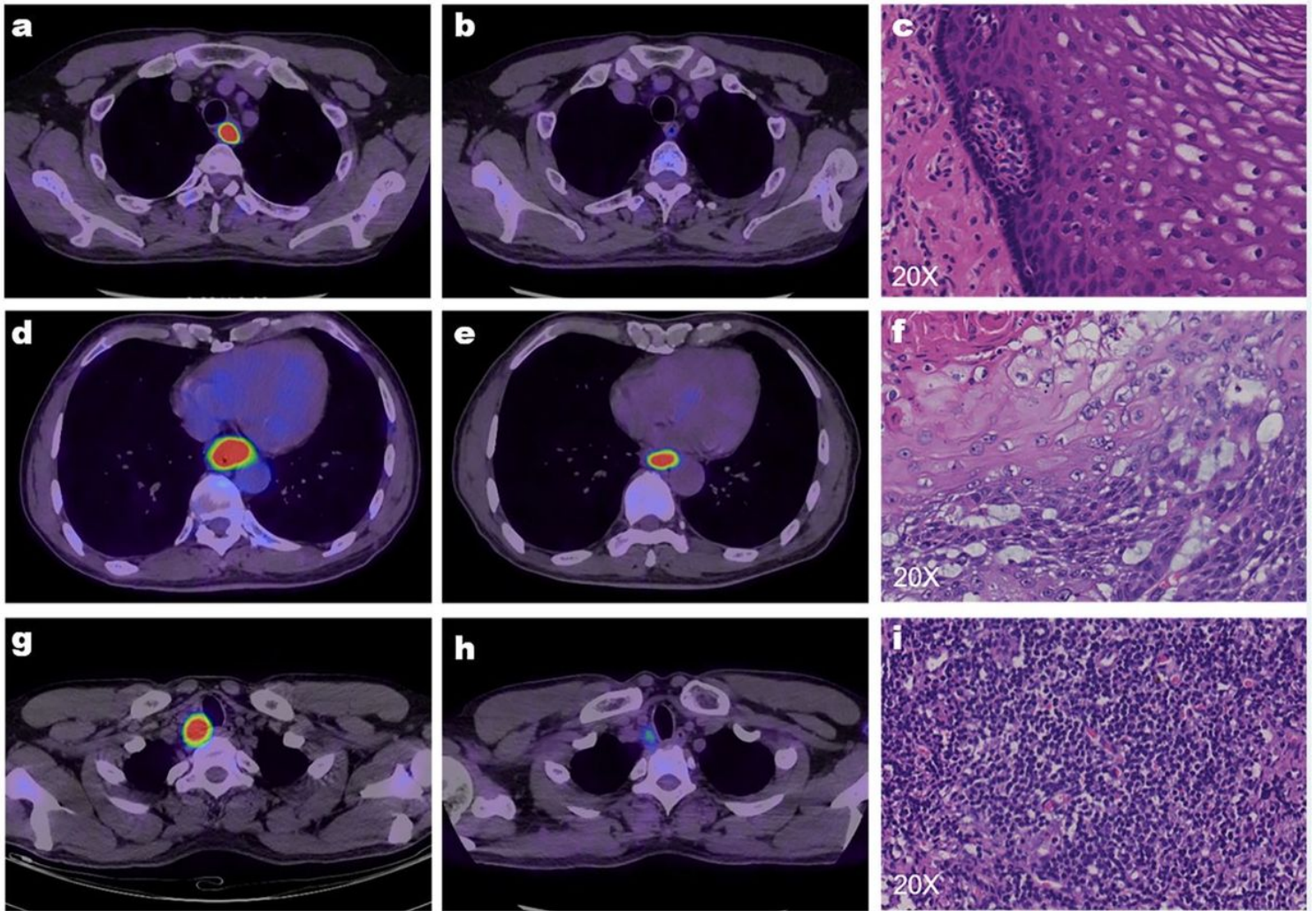
Figure 2

Two representative cases for patient with tumor pCR or non-pCR and one representative case for false-positive lymph node in ^{18}F-FDG PET/CT imaging. **a-c** A 59-year-old man with upper esophagus carcinoma who achieved pathological complete response after two cycles of immunochemotherapy. **a** Axial fusion image of scan-1, SUV_{max}=10.4, SUV_{mean}=14.6, TLG=29.0, MTV=2.0. **b** Axial fusion image of scan-2, SUV_{max}=2.9, SUV_{mean}=1.7, TLG=0.0, MTV=0.0. **c** Resection specimen (hematoxylin and eosin stain; magnification, 20×) showed that this patient had pCR (without viable tumor cells). **d-f** A 63-year-old man with lower esophagus carcinoma who achieved pathological partial response after two cycles of immunochemotherapy. **d** Axial fusion image of scan-1, SUV_{max}=13.9, SUV_{mean}=13.7, TLG= 239.6, MTV=19.1. **e** Axial fusion image of scan-2, SUV_{max}=13.9, SUV_{mean}=8.7, TLG=37.5, MTV=4.7. **f** Resection specimen (hematoxylin and eosin stain; magnification, 20×) showed that esophageal squamous cell tumors infiltrated the muscularis propria. **g-i** A 45-year-old man with middle esophagus carcinoma who had pathological complete response after two cycles of immunochemotherapy. **g** Axial fusion image of scan-1, a right upper paratracheal node was deemed to be positive (SUV_{max}=16.2, SAD=21.0mm). **h** Axial fusion image of scan-2, right upper paratracheal nodes were deemed to be positive (SUV_{max}=3.0, SAD=11.0mm). **i** Resection specimen (hematoxylin and eosin stain; magnification, 20×) did not show any cancer cell metastasis.

Supplementary Files

This is a list of supplementary files associated with this preprint. Click to download.

- supplementalmaterial.docx